

Dark matter searches with Solar gamma rays using the *Fermi*-LAT

Davide Serini ^{a,*} **Mario Giliberti** ^{a,b} **Francesco Loparco** ^{a,b} and **Mario Nicola Mazziotta** ^a for the *Fermi*-LAT collaboration

^a*Istituto Nazionale di Fisica Nucleare, Sezione di Bari
via Orabona 4, I-70126 Bari*

^b*Dipartimento di Fisica “M. Merlin”, dell’Università e del Politecnico di Bari
via Amendola 173, I-70126 Bari, Italy*

E-mail: davide.serini@ba.infn.it

Dark matter (DM) particles in our Galaxy can be gravitationally trapped by the Sun. Their annihilation and decay can lead to final states with Standard Model (SM) particles, including gamma rays. In a possible scenario, DM particles can be captured in external orbits. In this case, gamma rays produced in DM annihilations and decays can be detected on Earth. In another possible scenario, DM particles are accumulated in the Solar core. In this case, their annihilation/decay products will likely be absorbed in the Sun. However, in this framework, some theoretical scenarios suggest that DM particles can annihilate into long-lived mediators, which are able to escape from the Sun and decay into final state with gamma rays detectable on Earth. All these processes would result in an excess in the gamma-ray spectrum from the Sun. We have analyzed a set of gamma-ray data collected by the *Fermi* Large Area Telescope (LAT) during its first 13.5 years of operation to search for possible excesses in the Solar spectrum. Since no excess is found, we set constraints on the DM-nucleon scattering cross-sections.

38th International Cosmic Ray Conference (ICRC2023)
26 July - 3 August, 2023
Nagoya, Japan



*Speaker

1. Introduction

Several experimental pieces of evidence suggest that the majority of the mass in our Universe is composed of non-baryonic dark matter (DM) [1]. Among the various DM candidates that arise in theories beyond the Standard Model (SM), Weakly Interacting Massive Particles (WIMPs) represent a promising class that fit within observational constraints. The indirect DM detection strategy relies upon searching for cosmic radiation resulting from the annihilation or decay of DM into SM particles within the regions with anticipated high DM abundance. In particular, if WIMPs annihilate or decay into gamma rays, these emissions can be detected by the *Fermi* LAT, providing indirect evidence for the existence of DM particles.

The Sun represents a promising target for indirect DM searches since DM particles from the Galactic halo can interact with Solar nuclei, are become gravitationally trapped. Consequently, the excess of DM particles can lead to their annihilation and subsequent production of SM particles, such as gamma rays. To constrain the DM signal from the Sun, the *Fermi*-LAT collaboration conducted a series of analyses by directly observing the Solar gamma-ray emission [2, 3] and implementing dedicated strategies to search for possible DM signals, including line-like, box-like, or continuum signals, in the energy spectra of gamma rays originating from the Sun. In 15 years of data collected by the LAT, no statistically significant features have been detected in the Sun's gamma-ray energy spectrum. Therefore, the analyses have provided constraints on both the spin-dependent and spin-independent DM-nucleon scattering cross-sections within a DM mass range from a few GeV up to a few tens of TeV.

2. Solar dark matter models

The search for DM gamma rays originating from the Sun is a highly promising channel for indirect investigation. In one potential scenario, a DM particle, χ , undergoes inelastic scattering with Solar nuclei and is captured after a few interactions. In this model, the captured particles do not thermalize and settle in the Sun's core, but instead orbit around it. The direct annihilations of trapped DM particles can generate an observable flux of gamma rays from the Sun ($\chi\chi \rightarrow \gamma\gamma$), resulting in a characteristic line-like feature in the energy spectrum detected on Earth at an energy corresponding to the mass of the DM particle, m_χ [2, 4].

On the other hand, if DM particles are captured by the Sun through elastic scattering interactions with Solar nuclei, they can lose energy in subsequent interactions until they sink into the Sun's core, reaching thermal equilibrium. In this case, among the possible DM annihilation products, only low-energy neutrinos can escape from the Sun, while gamma rays or electron-positron pairs are likely to be absorbed and remain undetected on Earth. However, as proposed in [5–8], DM particles in the Solar core can also annihilate into long-lived mediators ϕ ($\chi\chi \rightarrow \phi\phi$), which can escape from the Sun and subsequently decay, producing detectable gamma rays as signatures of DM. If the mediator decays directly into gamma-ray pairs through the process $\phi \rightarrow \gamma\gamma$, and under the assumptions of DM particles annihilating at rest and light mediators ($m_\phi \ll m_\chi$), the resulting gamma ray spectra from DM are expected to exhibit a box-like feature [2, 9]. The upper edge of the box corresponds to the mass m_χ of the candidate DM particle [10].

Conversely, if gamma rays are produced in the final state through mediator decays (e.g. as final state radiation through the decay channels $\phi \rightarrow b\bar{b}, \tau^+\tau^-, \mu^+\mu^-, \dots$), the DM gamma-ray spectrum is predicted to have a smooth shape, depending on the masses of both DM and the mediator, as well as the explored decay channel of the mediator [3, 11].

In all the possible scenarios presented, the number of DM particles in the Sun at a given time, $N_\chi(t)$, can be determined by solving the balance equation $\frac{dN_\chi}{dt} = \Gamma_{\text{cap}} - C_{\text{ann}}N_\chi^2$ ¹. Here, Γ_{cap} represents the DM capture rate, and C_{ann} is the DM annihilation factor dependent on the annihilation cross section. At equilibrium, when $dN_\chi/dt = 0$, the annihilation rate becomes independent of the annihilation cross section and is set by the capture rate Γ_{cap} :

$$\Gamma_{\text{ann}} = \frac{1}{2}C_{\text{ann}}N_\chi^2 = \frac{1}{2}\Gamma_{\text{cap}}. \quad (1)$$

The factor of 1/2 accounts for the two DM particles involved in each annihilation event and the capture rate depends on the scattering cross section (either spin-dependent or spin-independent), the local halo DM number density ρ_\odot , the DM mass m_χ , the DM velocity distribution, and its dispersion. In the general case in which the equilibrium between capture and annihilation is not achieved, the general solution of the balance equation is given by $N_\chi(t) = \sqrt{\frac{\Gamma_{\text{cap}}}{C_{\text{ann}}}} \tanh\left(\frac{t}{\tau}\right)$ where $\tau = (\Gamma_{\text{cap}}C_{\text{ann}})^{-1/2}$ is the equilibrium time scale of the process [13]. As a consequence, the annihilation rate in Eq. 1 should be multiplied by the factor $\tanh^2(t/\tau)$.

2.1 Gamma rays from Solar dark matter

In the framework of DM annihilation through a mediator stage ($\phi \rightarrow b\bar{b}, \tau^+\tau^-, \mu^+\mu^-, \dots$) with final state radiation (FSR), the expected gamma-ray spectrum will extend up to the DM particle mass m_χ and expected DM gamma-ray flux at Earth Φ_{DM} can be written as [3]:

$$\Phi_{\text{DM}}(E; m_\chi, m_\phi, \sigma, L) = \Gamma_{\text{cap}}(m_\chi, \sigma) \cdot \varphi(E; m_\chi, m_\phi, L). \quad (2)$$

The term $\varphi(E; m_\chi, m_\phi, L)$ represents the flux of gamma rays per DM annihilation as observed on Earth that depends on the masses m_χ and m_ϕ , as well as the mediator decay length L . This term can be expressed as:

$$\varphi(E; m_\chi, m_\phi, L) = \frac{1}{4\pi D^2} Y(E; m_\chi, m_\phi, L) \quad (3)$$

where $D = 1$ AU denotes the Sun-Earth distance, and $Y(E; m_\chi, m_\phi, L)$ represents the gamma-ray yield per DM annihilation, which depends on the kinematics of the mediator decay². It is important to note that Eq. 2 implicitly assumes the equilibrium between the DM capture and annihilation processes [3].

In the particular case in which DM-particle annihilation occurs via a light intermediate state ($m_\phi \ll m_\chi$) that decays directly into photons ($\chi\chi \rightarrow \phi, \phi \rightarrow \gamma\gamma$) the expected DM gamma-ray flux on Earth $\Phi_{\text{DM}}(E)$ can be described as [2, 14]:

$$\Phi_{\text{DM}}(E) = N_\gamma(E) \frac{\Gamma_{\text{cap}}}{4\pi D^2} \left(e^{-R_\odot/L} - e^{-D/L} \right) \quad (4)$$

¹We have omitted the evaporation mechanism which is negligible for DM masses above a few GeV [7, 12].

²In this formulation, the mass m_χ of the parent DM particle sets the energy of the mediator in the lab frame, assuming the annihilation process $\chi\chi \rightarrow \phi\phi$ occurs with both DM particles at rest.

where R_\odot is the Solar radius and $N_\gamma(E)$ is the spectrum of photons produced by the mediator decay. Since the process $\phi \rightarrow \gamma\gamma$ is a two-body decay, $N_\gamma(E)$ will have a box-like shape and, if $m_\phi \ll m_\chi$, the box will extend from $E = 0$ to $E = m_\chi$ [10].

The DM capture rate Γ_{cap} is determined using the DARKSUSY code³ [15, 16]. The capture rate is evaluated for both the spin-dependent and spin-independent cases using a reference cross section of $\sigma_0 = 10^{-40} \text{ cm}^2$. The linear dependence of the capture rate on the DM-nucleon cross section allows for an easy computation of capture rates corresponding to different cross sections.

To evaluate the gamma-ray yields $Y(E; m_\chi, m_\phi, L)$ term in Eq. 3 for various mediator decay channels, we perform a dedicated simulation campaign [3] using the WimpSim code [17]. The DM annihilations are simulated using the event generator Pythia-6.4.26 [18], which also account for the subsequent decay chains of the annihilation products, considering the survival probability of the mediator during its journey from the Sun to the Earth.

3. Data Analysis

The Sun is a bright source of gamma rays, due to the interactions of cosmic rays (CRs) with the Solar environment [19, 20]. Any possible DM signal will, therefore, appear as an excess over the steady gamma-ray emission spectrum that represents the relevant background for DM searches. Modeling the steady Solar gamma-ray emission is not straightforward and, although several attempts were performed in the past following different approaches [21, 22], none of these models accurately reproduces the gamma-ray flux measured by the *Fermi* LAT.

The strength of LAT data analyses presented in this paper [2, 3] is that they are based on different strategies that do not require any template model for the standard Solar emission. All the analyses presented in this paper has been performed using an on/off technique, in which from the LAT data are selected photons with energies above 100 MeV from a Region of Interest (RoI) centered on the Sun (“on region”) combined with those from a RoI centered on the anti-Sun (“off region”). The direction of the anti-Sun is defined as the direction of the Sun with a forward/backward time offset of 6 months⁴ (for a complete description of data selection refers to [2, 3]).

3.1 Search for local excess in the gamma-ray emission towards the Sun

Since the DM scenarios illustrated above are expected to exhibit a distinct spectral feature in the Solar gamma-ray energy spectrum (line-like and box-like features), we implemented a Poisson maximum likelihood fitting procedure in order to search for possible local excesses in the photon count spectra [2]. The fits are performed scanning the entire data sample in sliding energy windows ranging from 100 MeV to 150 GeV to search for DM signatures that would result in local excess counts above a smooth spectrum⁵. For the fits, flux models are defined for both the “on” and “off”

³<http://www.darksusy.org/>

⁴This choice ensures that the angular separation between the Sun and the anti-Sun is always close to 180° and that, during the LAT data-taking, the anti-Sun follows the same path in the sky as the Sun. The off region is therefore an optimal control region to take into account any possible systematic uncertainties.

⁵Each energy window is defined as the interval $[(1-w)E_w, (1+w)E_w]$, where E_w is the energy corresponding to the center of the window and wE_w is the half-width of the window. The parameter w is fixed to 0.6 and it is chosen in order to ensure that the width of the windows is larger than the LAT energy resolution for the whole energy range explored in the analysis.

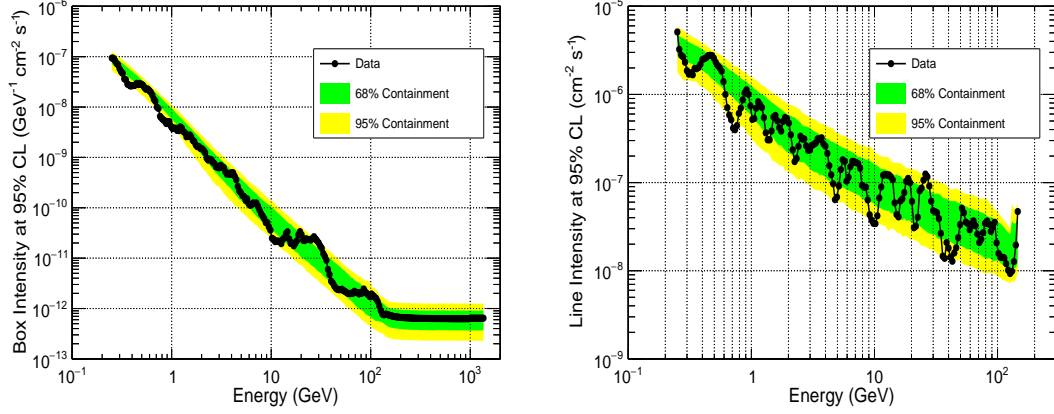


Figure 1: Upper limit at 95% confidence level on the intensity of the feature in the Solar spectrum. Left panel: box model; Right panel: line model. The green and yellow regions represent the central 68% and 95% expectation bands, respectively, for the 95% CL limits. Adapted from [2].

regions, and the fitting procedure determines the best-fit parameters for the assumed models. In each region, the flux contributions can be expressed as the sum of a continuous smooth component, $\Phi_0(E)$, and a potential additional feature, $\Phi_f(E)$, that is being sought. The continuous term represents the net signal flux from the Sun, $\Phi_{\text{sig}}(E_t)$, contributing only in the "on" region, while an additional background flux, $\Phi_{\text{bkg}}(E_t)$ (including diffuse, point sources, and irreducible background), contributes in both the on and off regions. Since we use narrow energy windows, the continuous terms in the flux models can be well described by a simple power law model. For the spectral feature $\Phi_f(E; s)$, two different models are assumed. A delta-like (line) feature, $\Phi_f(E; s) = s \delta(E_f - E)$, and a box-like (box) feature $\Phi_f(E; s) = s H(E_f - E)$, where E_f is the characteristic energy of the feature (either the line energy or the upper edge of the box), δ is the Dirac delta function, H is the Heaviside step function and s represents the intensity of the feature. To assess the significance of a signal feature, the local Test Statistic, $TS = 2\Delta \log \mathcal{L} = 2(\log \mathcal{L}_1 - \log \mathcal{L}_0)$, is calculated, where \mathcal{L}_0 and \mathcal{L}_1 are the likelihood function values obtained when fitting the data with the models corresponding to the null hypothesis (i.e., no feature included) and the alternative hypothesis (i.e., feature included), respectively.

Fig. 1 shows the upper limits (ULs) at a 95% confidence level (CL) on the intensity of both the box-like and line-like features. The plots display the central 68% and 95% containment bands for the ULs, which are evaluated from the pseudo-experiments. It can be observed that the measured upper limits for both types of features fall within the central 95% expectation band.

3.2 Search for extended DM signatures in the Solar gamma-ray spectrum

In the framework of DM annihilation through a mediator stage with FSR, the expected DM gamma-ray signature in the Solar spectrum extends across a broad energy range. To analyze the LAT data without relying on a template model for the standard Solar emission, two different approaches are used [3]. In the first approach, all the excess counts in the on region relative to the off region are assumed to entirely originate from DM signal. In this case, the upper limits on the DM-nucleon cross section obtained will be overestimated since the steady Solar emission is neglected (“conservative

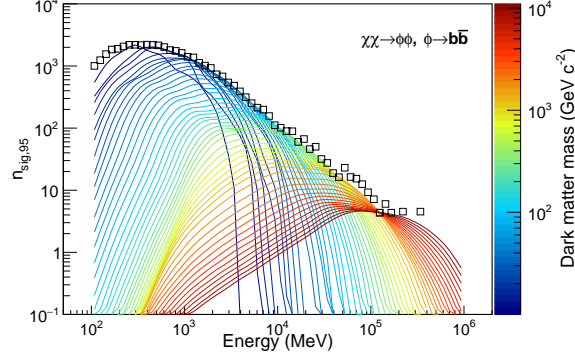


Figure 2: Upper limits (95% CL) on DM gamma-ray fluxes using a conservative approach. The plot shows results for the mediator decay channel $\phi \rightarrow b\bar{b}$ with $m_\phi = 11.5 \text{ GeV}c^{-2}$. Open squares represent upper limits (95%CL) on signal counts $n_{sig,95}(E_o)$ [23]. Each colored line corresponds to the upper limit on DM gamma-ray counts for a specific DM mass m_χ . The color scale on the right indicates the values of m_χ . Adapted from [3]

approach”). On the other hand, in the second approach, the excess counts in the on region are attributed to the steady Solar emission, while gamma rays from DM annihilations are considered responsible only for potential fluctuations in these excess counts. Therefore, using this second approach, the constraints on the DM-nucleon cross sections will be stronger compared to the first approach (“optimistic approach”). For each decay channel and for each pair of masses (m_χ, m_ϕ) , the DM gamma-ray flux is modeled as: $\Phi_{DM}(E) = k_{DM}\Phi_{DM,0}(E; m_\chi, m_\phi, \sigma_0, R_\odot)$ where the flux $\Phi_{DM,0}(E; m_\chi, m_\phi, \sigma_0, R_\odot)$ (see Eq. 2) is evaluated using a reference cross-section value of $\sigma_0 = 10^{-40} \text{ cm}^2$, assuming a mediator decay length $L = R_\odot$. The reference fluxes are evaluated for different mediator decay channels using the simulation results performed with WimpSim (Sec. 2.1), covering a wide range of DM masses and mediator masses. Figure 2 shows an example of application of this approach to evaluate the upper limits at 95% CL on the DM gamma-ray fluxes in the scenario of the mediator decay channel $\phi \rightarrow b\bar{b}$, assuming $m_\phi = 11.5 \text{ GeV}c^{-2}$.

4. Results and conclusions

In this paper, we report the recent results from the *Fermi*-LAT Collaboration in the DM physics searching for signature in the gamma-ray spectrum toward the Sun as indirect probe of WIMPs [2, 3]. No statistically significant features have been detected in the energy spectra through various analyses. The limits on the intensity of these features are used to constrain both the spin-dependent and spin-independent DM-nucleon scattering cross sections in a DM mass range from a few GeV up to several TeV. The limits obtained within the mediator scenario are presented in Fig. 3 for the search of box-like features. The left panel shows the limits assuming equilibrium between DM capture and annihilation in the Sun, while the right panel includes limits for both the equilibrium and non-equilibrium setups, where a velocity-averaged cross section at the thermal relic value of $\langle\sigma_{ann}v\rangle = 3 \times 10^{-26} \text{ cm}^3/\text{s}$ is assumed [26]. Figure 4 shows the limits obtained by considering various mediator decay channels with gamma rays produced in the final state, for both the spin-dependent and spin-independent DM-nucleon scattering cross sections, σ_{SD} and σ_{SI} respectively.

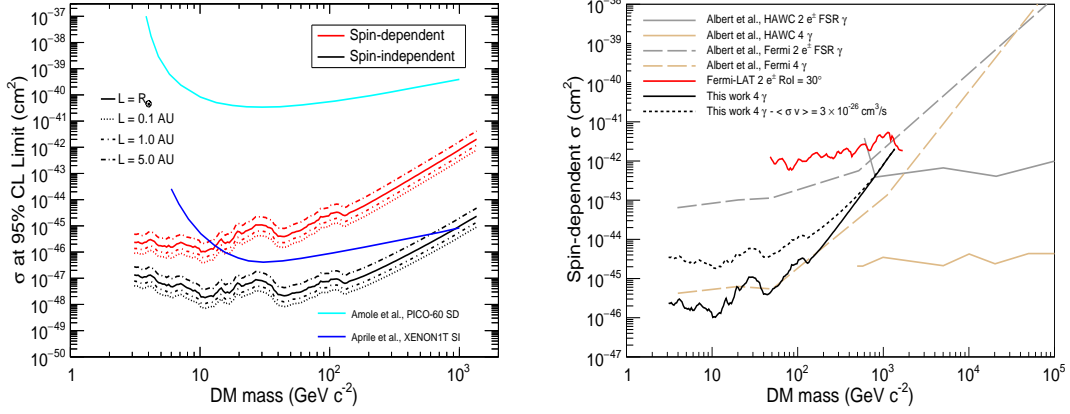


Figure 3: *Left panel:* Upper limits at 95% CL on the DM-nucleon cross section for long-lived mediators with different decay lengths ($L = R_\odot, 0.1, 1$ and 5 AU). The limits at 90% CL from the PICO-60 experiment (cyan line) for spin-dependent scattering [24] and from the XENON1T experiment (blue line) for spin-independent scattering [25] are also shown. *Right panel:* Upper limits at 95% CL on the spin-dependent DM-nucleon scattering cross section for the long-lived mediator with decay length $L = R_\odot$, compared with the limits obtained from HAWC and *Fermi* [7], and with the *Fermi*-LAT results obtained with CR electrons [8]. Adapted from [2].

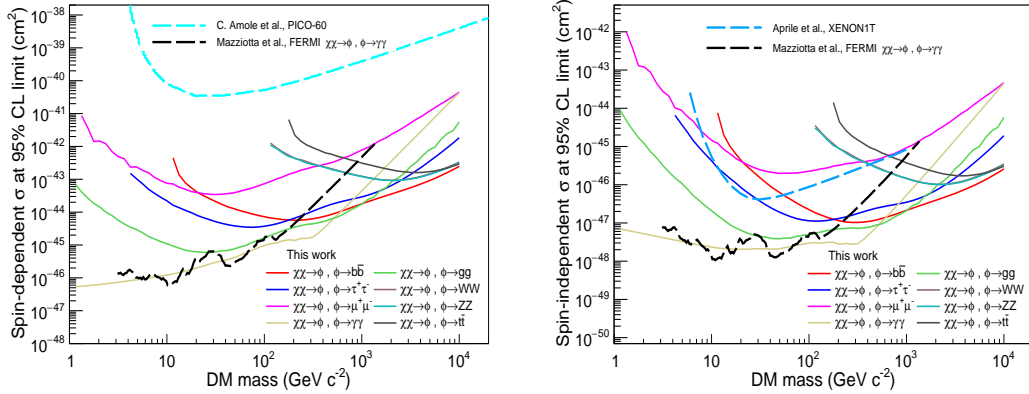


Figure 4: Upper limits (95% CL) on spin-dependent (left) and spin-independent (right) DM-nucleon scattering cross-sections for DM annihilating into long-lived mediators. Channels include $b\bar{b}$, $\tau^+\tau^-$, $\mu^+\mu^-$, $\gamma\gamma$, gg , WW , ZZ , and $t\bar{t}$, with $L = R_\odot$. The 90% CL limits obtained from PICO-60 [24] (spin-dependent) and XENON1T [25] (spin-independent) experiments are also shown. Adapted from [3].

All these results are compared with direct measurements conducted by the XENON1T [25] and PICO-60 [24] experiments, as well as with other experiments investigating the same theoretical scenario [7]. The obtained results demonstrate the potential of Solar gamma rays as a probe for indirect DM detection, with comparable or even stronger limits than those reported in the current literature.

Acknowledgments

The *Fermi*-LAT Collaboration acknowledges support for LAT development, operation and data analysis from NASA and DOE (United States), CEA/Irfu and IN2P3/CNRS (France), ASI

and INFN (Italy), MEXT, KEK, and JAXA (Japan), and the K.A. Wallenberg Foundation, the Swedish Research Council and the National Space Board (Sweden). Science analysis support in the operations phase from INAF (Italy) and CNES (France) is also gratefully acknowledged. This work performed in part under DOE Contract DE-AC02-76SF00515.

References

- [1] Tanabashi, M. et al., *Phys. Rev.*, (2018), **D98**, 030001
- [2] Mazziotta, M.N. et al., *Phys. Rev.*, (2020), **D102**, 022003
- [3] Serini D. et al., *JCAP* (2022), **02**, 025
- [4] Serini, D., Loparco, F. and Mazziotta, M.N, *PoS*, (2020), **ICRC2019**, 544
- [5] Schuster, P., Toro, N. and Yavin, I., *Phys. Rev.* (2010), **D81**, 016002
- [6] Leane, R.K., Ng, Kenny C. Y. and Beacom, J.F. *Phys. Rev.* (2017), **D95** 123016
- [7] Albert, A. et al., *Phys. Rev.*, (2018), **D98**, 123012
- [8] Mazziotta, M.N. et al., *Phys. Rev.*, (2018), **D98**, 022006
- [9] Loparco, F., Serini, D. and Mazziotta, M.N, *PoS*, (2021), **ICRC2021**, 513
- [10] Ibarra, A., Gehler, S.L. and Pato, M. *JCAP* (2012), **07**, 043
- [11] Serini, D., *J. Phys. Conf. Ser.*, (2023), **2429**, 012018
- [12] K. Griest and D. Seckel, *Nucl. Phys.*, (1987), **B283**, 681-705
- [13] G. Jungman, et al., *Phys. Rep.*, (1996), **267** , 195-373
- [14] A. Cuoco, et al., *Phys. Rev.*, (2020), **D101** (2020), 022002
- [15] P. Gondolo, et al., *JCAP*, (2004), **0407** (2004), 008
- [16] T. Bringmann, et al., *JCAP*, (2018), **1807** (2018), 033
- [17] Niblaeus, C., Beniwal, A. and Edsjö, J., *JCAP*, (2019), **11**–011
- [18] Sjöstrand, T., et. al., *Comput. Phys. Commun.*, (2015), **191**, 159–177
- [19] Abdo, A. A. et. al. *Astrophys. J.*, (2011) **734**, 116
- [20] Orlando, E. and Strong, A., *Astron. Astrophys.*, (2008), **480** 847
- [21] Moskalenko, I. V., Porter, T. A. and Digel, S. W., *Astrophys. J. Lett.*, (2006), **652**, 65–68
- [22] Mazziotta, M.N. et. al., *Phys. Rev. D*, (2020), **101** 083011
- [23] Loparco, F. and Mazziotta, M. N., *arXiv*, (2009), **0912.3695**
- [24] Amole C. et al., *Phys. Rev.*, (2019), **D100**, 022001
- [25] Aprile E. et al., *Phys. Rev. Lett.* (2018), **121**, 111302
- [26] G. Steigman, et. al., *Phys. Rev.*, (2012), **D86**, 023506